PROCEEDINGS OF SPIE

SPIEDigitalLibrary.org/conference-proceedings-of-spie

Assessing drug-cell and drug-tissue interactions through spectral FRET imaging

Leavesley, Silas, Annamdevula, Naga, Geurts, Aron, Pleshinger, D. J., Rich, Thomas

Silas J. Leavesley, Naga A. Annamdevula, Aron Geurts, D. J. Pleshinger, Thomas C. Rich, "Assessing drug-cell and drug-tissue interactions through spectral FRET imaging," Proc. SPIE 11624, Visualizing and Quantifying Drug Distribution in Tissue V, 116240D (5 March 2021); doi: 10.1117/12.2583249



Event: SPIE BiOS, 2021, Online Only

Assessing drug-cell and drug-tissue interactions through spectral FRET imaging

Silas J. Leavesley^{1,2,3}, Naga Annamdevula^{2,3}, Aron Geurts⁴, DJ Pleshinger^{2,3}, Thomas C. Rich^{2,3}

¹Chemical and Biomolecular Engineering, University of South Alabama, AL 36688

²Pharmacology, University of South Alabama, AL 36688

³Center for Lung Biology, University of South Alabama, AL 36688

⁴Physiology, Medical College of Wisconsin, WI 53226

ABSTRACT

Structural complexity and heterogeneity may play critical roles in pathophysiology and therapeutic effect, at length scales ranging from subcellular (nm) to whole organ (cm). Standard evaluation of pharmacologic agent-tissue interactions involves dose-dependent characterization of cellular physiology, and often spatial and temporal characterization of diffusion and kinetics. However, structural heterogeneity and intracellular signaling protein distribution may also drive physiologic responses. In prior work, we utilized Förster resonance energy transfer (FRET) reporters to visualize 3dimensional spatial distributions of the second messenger, cAMP. Results demonstrate that a combined spectral imaging - linear unmixing - image analysis approach allows visualization cAMP spatial distributions, and that unique spatial patterns are formed in a treatment-specific manner. Here, we report on efforts to expand this approach for visualization of the effects of pharmacologic treatments on tissues. In specific, we have developed a transgenic rat line using the "H187" cAMP FRET reporter expressed under the control of the Rosa26 locus for pan-cellular visualization of second messenger signaling in tissues in response to treatment and pathological conditions. When utilized with vascular and lung preparations, transgenic FRET tissues displayed the ability to elicit agonist-induced cAMP responses in single cells. At the tissue scale, this approach allows assessment of agonist diffusion and signaling kinetics, as well as cell-specific and intracellularly-localized events. Hence, when coupled with appropriate imaging platforms and image analysis algorithms, FRET reporters expressed in transgenic models allow visualization of the heterogeneous response to pharmacologic and pathologic stimuli at multiple length scales, from ~0.2 nm to cm in tissues.

Keywords: Spectral, Spectroscopy, Signature, Fingerprint, cyclic nucleotide, cAMP, second messenger

1. INTRODUCTION

Standard approaches for assessing response to pharmacologic agents in cells and tissues have utilized characterization strategies that commonly employ measurement of bulk cell and tissue properties as well as downstream physiology. These approaches have been critical for determining overall dose dependence and kinetics. However, more recent developments in cell signaling, such as in second messenger cyclic nucleotide signaling, have indicated that the spatial distribution (aka compartmentalization) of signaling agents, may play a key role in determining downstream physiology ^{1–3}. Adding to this complexity, subcellular compartmentalization of signals may occur in a manner that would not be supported assuming simple particle diffusion through the cytoplasm⁴. Hence, there is a need to further study and understand the complex and spatially-dependent signaling patterns that may arise in second messenger signaling, both at a subcellular length-scale as well as at tissue and organ length scales.

One tool that has aided in the study of cyclic nucleotide second messengers is the development of custom Förster resonance energy transfer (FRET) reporters that allow quantification of relative cyclic nucleotide concentration. In prior work, we have utilized the "H188" cAMP FRET reporter⁵ in combination with spectral imaging confocal microscopy to evaluate subcellular spatial distributions of cAMP within pulmonary microvascular endothelial cells⁶. We found that accounting for cellular autofluorescence and other background or interefering signals during the spectral unmixing process can improve the ability to quantitatively measure FRET efficiencies. This approach allowed us to visualize discrete subcellular cAMP distributions in 3 dimensions after a combined linear unmixing and image analysis pipeline.

Here, we present an extension of these efforts into the tissue level by combination of a novel cAMP reporter transgenic rat line and spectral imaging confocal microscopy. Our initial imaging attempts, described below, indicate that spectral imaging of FRET reporters in tissues is possible and that this approach should allow for measurement of spatially-resolved

Visualizing and Quantifying Drug Distribution in Tissue V, edited by Kin Foong Chan, Conor L. Evans, Proc. of SPIE Vol. 11624, 116240D ⋅ © 2021 SPIE CCC code: 1605-7422/21/\$21 ⋅ doi: 10.1117/12.2583249

cAMP dynamics within tissues, and possibly even entire organs or whole animals. However, much work is still needed to overcome limitations associated with the greatly increased and tissue-specific autofluorescence of tissues, as well as optical penetration, photobleaching, and agonist delivery challenges.

2. METHODS

2.1 Cell Culture

Human airway smooth muscle cells (HASMCs) were isolated and maintained in Dulbecco's Modified Eagles Medium (DMEM, Life Technologies, Inc.) supplemented with 10% v/v fetal bovine serum (Gemini), 0.5 μ g/L basic Fibroblast Growth Factor (bFGF), 2 μ g/L human Epidermal Growth Factor (EGF), 100 U/mL penicillin, and 100 μ g/mL streptomycin at pH 7.0. For imaging, cells were grown to 70-80% confluency on 25 mm, laminin-coated, round coverslips at 80 °F. Cells were transfected with pCDNA3 encoding the H188 FRET reporter two days prior to imaging. On the day of imaging, coverslips were transferred to an Attofluor cell chamber (ThermoFisher Scientific) and bathed in 800 μ L buffer. During imaging, at the desired time point, 200 μ L buffer containing either 0.1 μ M isoproterenol or 0.1 μ M PGE₁ was added to elicit cAMP response.

2.2 Transgenic Animal

All animal procedures were performed in accordance with approved Institutional Animal Care and Use Committee (IACUC) protocols. A novel transgenic rat that expressed the H187 FRET reporter was generated by Dr. Aron Geurts at the Medical College of Wisconsin. The FRET reporter was inserted into the Rosa26 locus, which is thought to be a site for ubiquitous expression, although this must still be confirmed with regards to this specific FRET reporter. On the day of imaging, animals were euthanized according to approved IACUC protocols and organs harvested. Kidney tissues were prepared by slicing into ~1 mm slices using a surgical knife. Kidney slices were then placed onto 25 mm round glass coverslip housed in an Attofluor, bathed in PBS, and imaged. Large vessels, including the inferior vena cava (IVC) were prepared by isolation of the vessel, longitudinal opening, and securing onto SYLGARD blocks. Vessel-block preparations were placed onto 25 mm round glass coverslips housed in an Attofluor and bathed in PBS with the intima facing downward (toward the coverslip and microscope objective). Vessels were separated from the glass coverslip using 100 μm spacers so as to allow diffusion of buffer and any agonist directly onto the endothelium. During imaging, at the desired time point, vessels were treated with 50 μM forskolin and 10 μM rolipram to elicit cAMP response.

2.3 Spectral Confocal Microscopy

Spectral imaging confocal microscopy was performed using an inverted A1R spectral confocal microscope (Nikon Instruments), as described previously⁶. In brief, samples were imaged using either 20X or 60X objectives with 405 nm excitation and spectral detection via a 32-channel detector. Image data were exported as a series of unscaled tiff files (one per channel) and processed using a custom MATLAB program for non-negatively-constrained least-squares linear unmixing, FRET quantitation, and visualization. FRET efficiency images were further processed to estimate a relative cAMP concentration, that is reported as a ratio of cAMP/K_d (dissociation constant of the cAMP FRET reporter). When appropriate, 3D image data of FRET or relative cAMP concentration were sliced and visualized along varying XY, XZ, and YZ planes to visualize FRET or cAMP signals within the respective planes. For single-plane kinetic analysis, time-lapse studies were performed at a plane of interest and FRET or cAMP signals were visualized as a function of time-point.

3. RESULTS AND DISCUSSION

3.1 Spatially-Localized cAMP Signals Within Airway Smooth Muscle Cells

Analysis of dynamic cAMP signals within HASMCs revealed that $0.1~\mu M$ isoproterenol treatment at a time point of 60 seconds resulted in biphasic cAMP response, with initial cAMP concentration increasing to a maximum at roughly a time point of 330 s, then decreasing, and then increasing to a higher maximum by the final time point of 1200 s (Figure 1). This biphasic response was seen in approximately 80-90% of experimental trials when treated with $0.1~\mu M$ isoproterenol. There also appears to be a slight apical-to-basal distribution of cAMP, that is best visualized at the 330 s time point in the YZ plane.

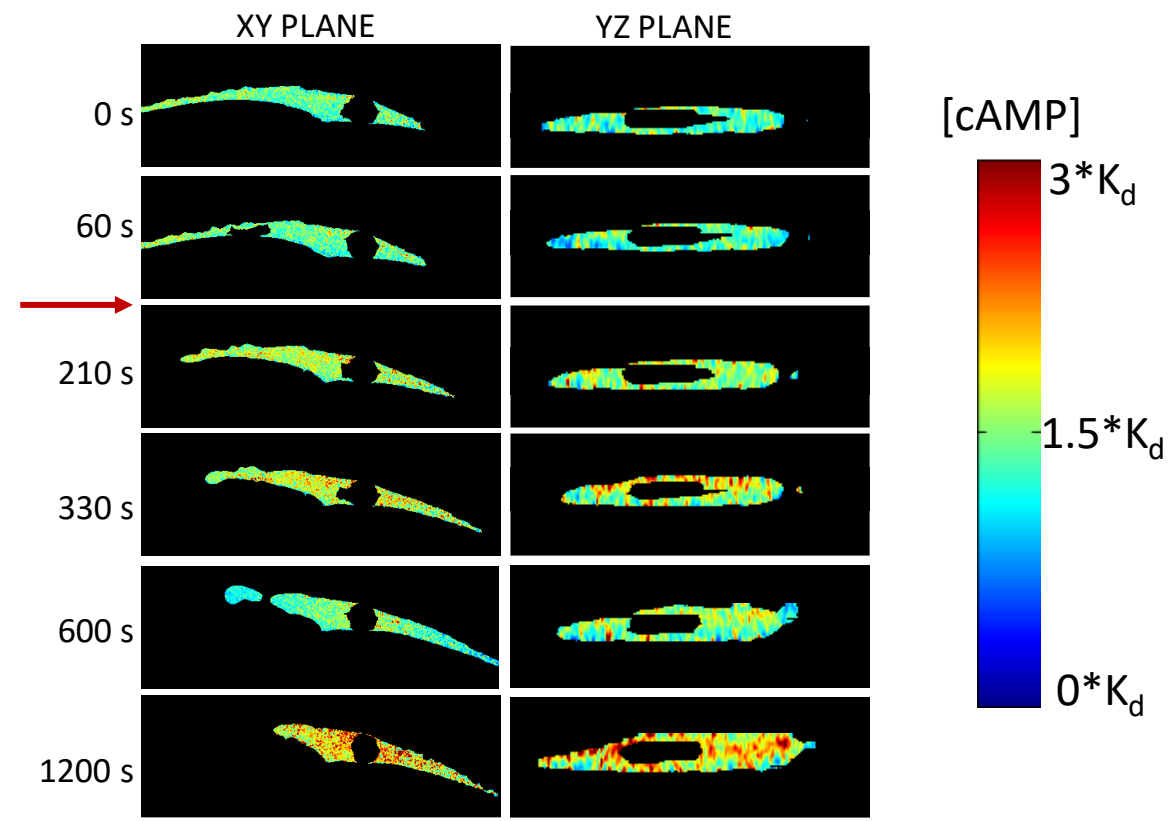


Figure 1: Timelapse spectral image data of a human airway smooth muscle cell (HASMC) expressing the H188 venus-turquoise cAMP FRET probe and treated with $0.1~\mu M$ isoproterenol after a time point of 60~s. The images in the left column display a standard lateral rendering (XY plane) of the image data while the images in the right column display an axial rendering (YZ plane). The heatmap indicates the cAMP concentration as normalized to the dissociation constant, K_d , of the H188 FRET reporter.

In contrast to the isoproterenol treatment described above, analysis of HASMCs treated with 0.1 µM PGE₁ produced a steady increase in cAMP that appeared to reach a maximum, or plateau, by 1200 s (Figure 2). In addition, there appeared to be small regions of localized increased cAMP ("hot spots") near the basal side of the cell. Hence, treatment with PGE₁ produced a cAMP response that was both temporally as well spatially variant from the response produced by isoproterenol, indicating the need for further study of spatially and temporally variant cAMP signaling to understand the role that these variations may (or may not) play in downstream cellular physiology and pathophysiology.

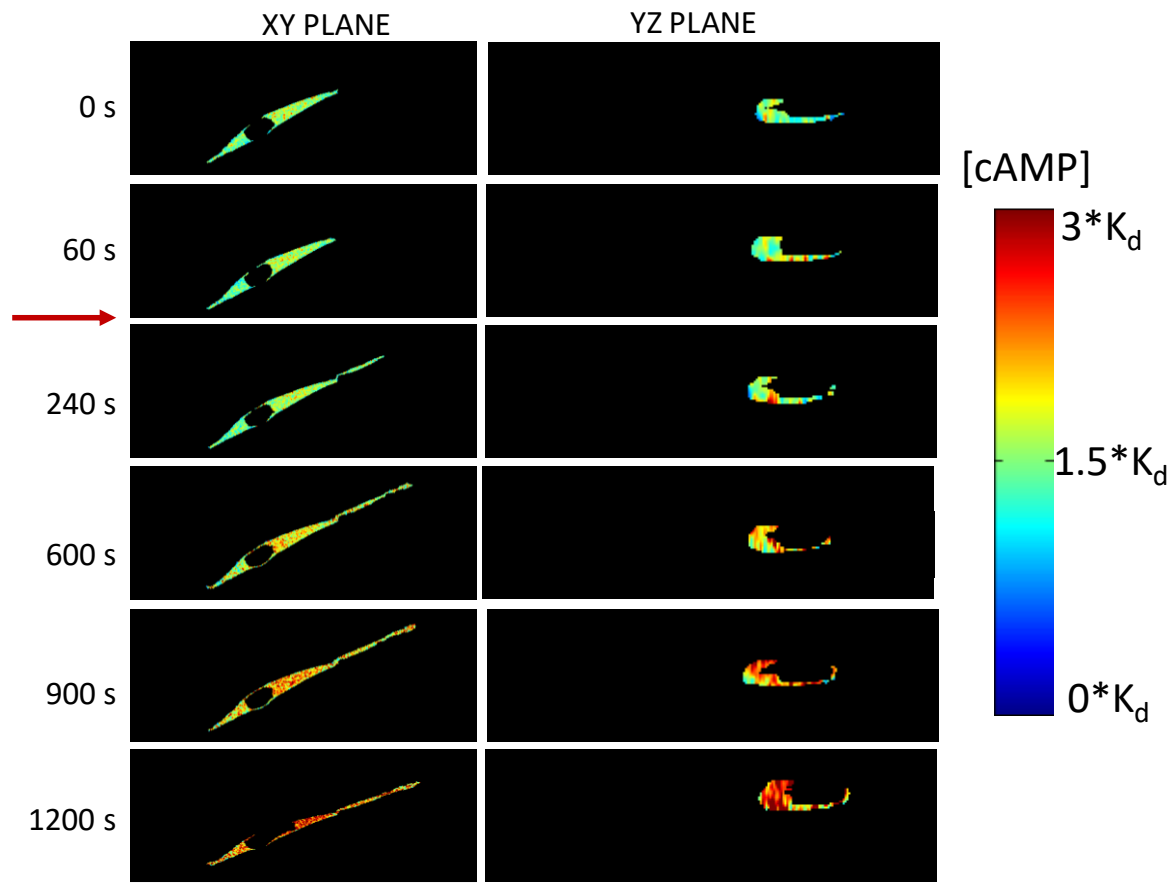


Figure 2: Timelapse spectral image data of a human airway smooth muscle cell (HASMC) expressing the H188 venus-turquoise cAMP FRET probe and treated with $0.1~\mu M$ PGE₁ after a time point of 60~s. The images in the left column display a standard lateral rendering (XY plane) of the image data while the images in the right column display an axial rendering (YZ plane). The heatmap indicates the cAMP concentration as normalized to the dissociation constant, K_d , of the H188 FRET reporter

3.2 Preliminary Tissue-Level cAMP FRET Imaging in Resected Tissues

The ability to detect the cAMP FRET reporter and to quantify changes in FRET (and hence, cAMP level) was assessed through use of a transgenic rat line that expressed the H187 cAMP FRET reporter. To first assess the ability to detect the FRET reporter, tissues were isolated from expressing and non-expressing (wildtype control) rats. Most tissues presented high levels of autofluorescence, for example, as associated with the convoluted tubules of the kidney (Figure 3, A-B). While we have previously shown that spectral imaging provides an avenue for separation of cellular autofluorescence and background signals from the desired donor and acceptor FRET signals^{6,7}, the autofluorescence signal levels encountered in whole tissue imaging were significantly higher than those encountered when imaging cell monolayers. Hence, these interfering signals greatly tested the ability of the spectral detection and analysis approach to accurately identify the donor and acceptor FRET signals. However, with careful and appropriate construction of a spectral library that included the autofluorescence spectrum of kidney from a wildtype control rat (Figure 3C), it was possible to linearly unmix the signals from each of the donor, acceptor, and autofluorescence, as well as to produce a false-colored overlay that allowed visualization of the donor and acceptor signals mixed with the autofluorescence. This process resulted in low unmixed signals from donor and acceptor in the wildtype control kidney tissue (Figure 3, D-G), as expected, and much higher donor and acceptor signals detected in kidney tissues resected from the transgenic H187 cAMP FRET rat (Figure 3, H-K). Hence, in principle, these initial results indicate that it is possible to detect and separate the donor and acceptor signals of the FRET probe from that of the autofluorescence, even when the magnitude of the autofluorescence signal appears as high or higher than the donor and acceptor signal.

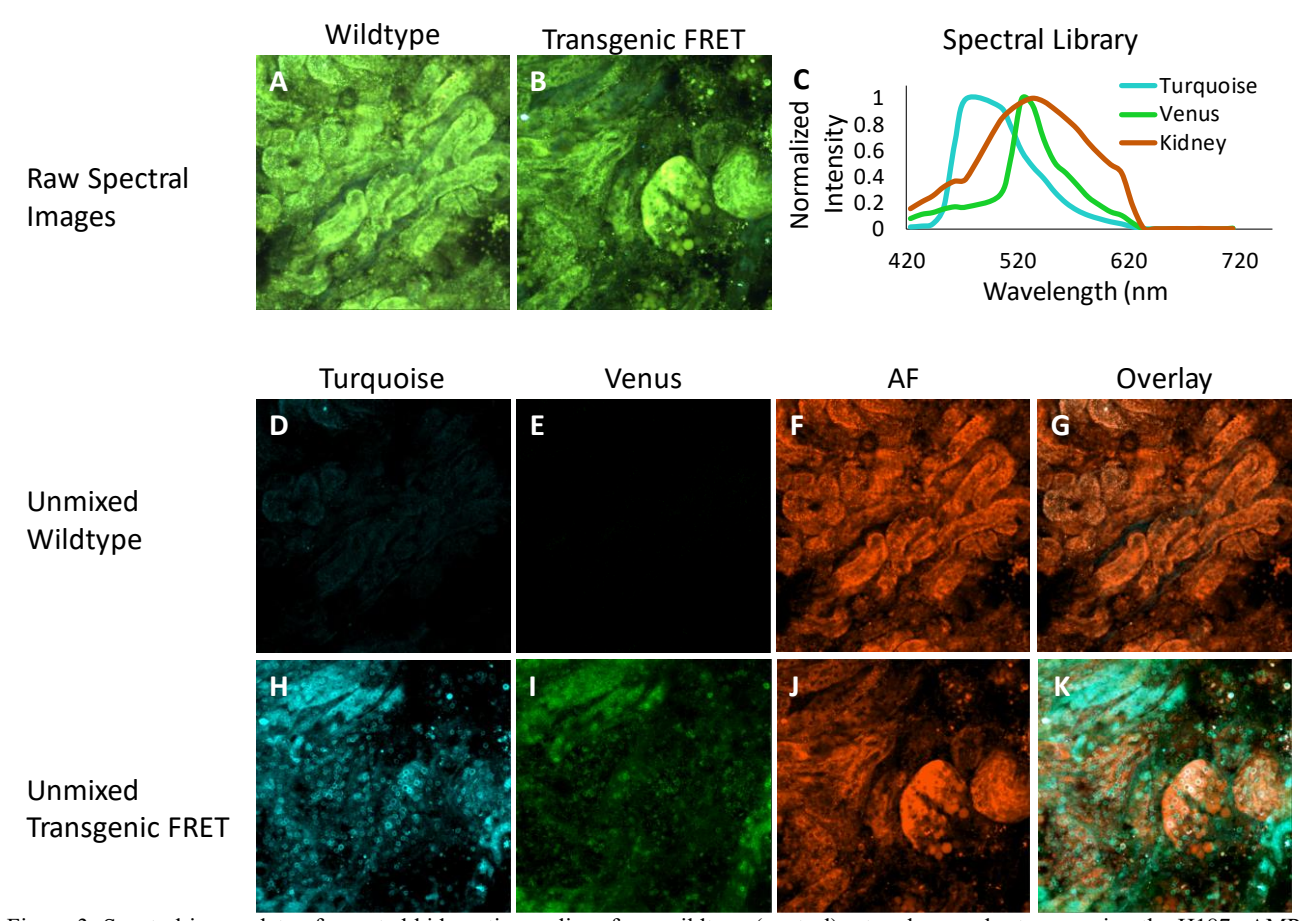


Figure 3: Spectral image data of resected kidney tissue slices from wildtype (control) rat and a novel rat expressing the H187 cAMP FRET reporter. Raw, false-colored spectral image data from wildtype (A) and transgenic (B) rat was unmixed using a spectral library (C) that was customized to the specific tissue type, in this case kidney. Unmixed images from wildtype rat kidney slices displayed low donor (turquoise, D) and acceptor (venus, E) signals, and were primarily autofluorescence (F). A false-colored overlay of unmixed signals (G) was generated to visualize localization of signals. Unmixed images from transgenic cAMP FRET rat kidney slices displayed appreciable levels of donor (H) and acceptor (I) signals, as well as autofluorescence (J). A false-colored overlay demonstrated that autofluorescence structures were different than structures labeled with the FRET probe, likely confirming the validity of unmixing results.

To further test the ability to detect changes in FRET level, and hence changes in cAMP level, in resected tissues, vessel preparations were imaged that allowed detection of FRET at the vessel endothelium while providing a small (100 μ m thick) region of buffer-filled space between the vessel endothelium and coverslip for diffusion of agonist in order to visualize dynamic cAMP responses. Early preliminary data from inferior vena cava (IVC) preparations displayed a high level of autofluorescence (Figure 4A, D), as was also seen in the kidney. Using a spectral library that included the autofluorescence spectrum of the IVC as obtained from tissues isolated from wildtype control animals, the donor, acceptor, and autofluorescence signals were linearly unmixed and the donor and acceptor signals were used to estimate a FRET index (the absolute FRET efficiency was not initially calculated due to the likely higher uncertainty of the calculations that was caused by high autofluorescence levels). Despite the very high autofluorescence that appears to be in large part due to the basal lamina, detection of the donor and acceptor in small patches of endothelium was possible (Figure 4, B-C). When treated with 50 μ M forskolin and 10 μ M rolipram to elicit cAMP response, the FRET index decreased as expected (Figure 4E). The FRET increase was further validated by plotting the individual donor and acceptor abundances over time, which indicated an increase in donor and decrease in acceptor, as would be expected to yield a decrease in FRET index (Figure 4F).

These initial results indicate that detection of changes in FRET index, and hence corresponding changes in cAMP, are possible within tissues and that with further work it should be possible to visualize spatial distributions or variations in cAMP levels within tissues, and ideally at the subcellular level within tissues. Unfortunately FRET signals, especially

those occurring due to fluorescent-protein based reporters, are often weak^{8,9} and it is difficult to detect FRET accurately, at subcellular length scales, and at temporal resolutions needed to resolve cAMP signaling dynamics. The hyperspectral imaging approach describes here lends spectral specificity to FRET detection, allowing the separation of cell and tissue autofluorescence from the donor and acceptor signals. Indeed, spectral imaging approaches have previously been demonstrated to be highly effective for separating signals from multiple labels as well as autofluorescence¹⁰, and for quantification of FRET efficiency^{11,12}. However, spectral imaging technologies, as implemented on confocal microscope platforms, typically involve use of a diffractive element, such as a grating or prism, that disperses the fluorescence emission spectrum onto a detector array, such as a multi-anode PMT array^{13,14}. While effective for measuring the resulting fluorescence emission spectrum, this optical implementation also has the effect of producing a relatively weak signal upon each detector element, because signal is distributed over the entire array of detector elements. Hence, there is an ongoing need for microscopic imaging technologies that provide both spectral specificity as well as high sensitivity and sufficient signal strength to allow for meaningful FRET measurements, especially when investigating kinetic responses in tissues.

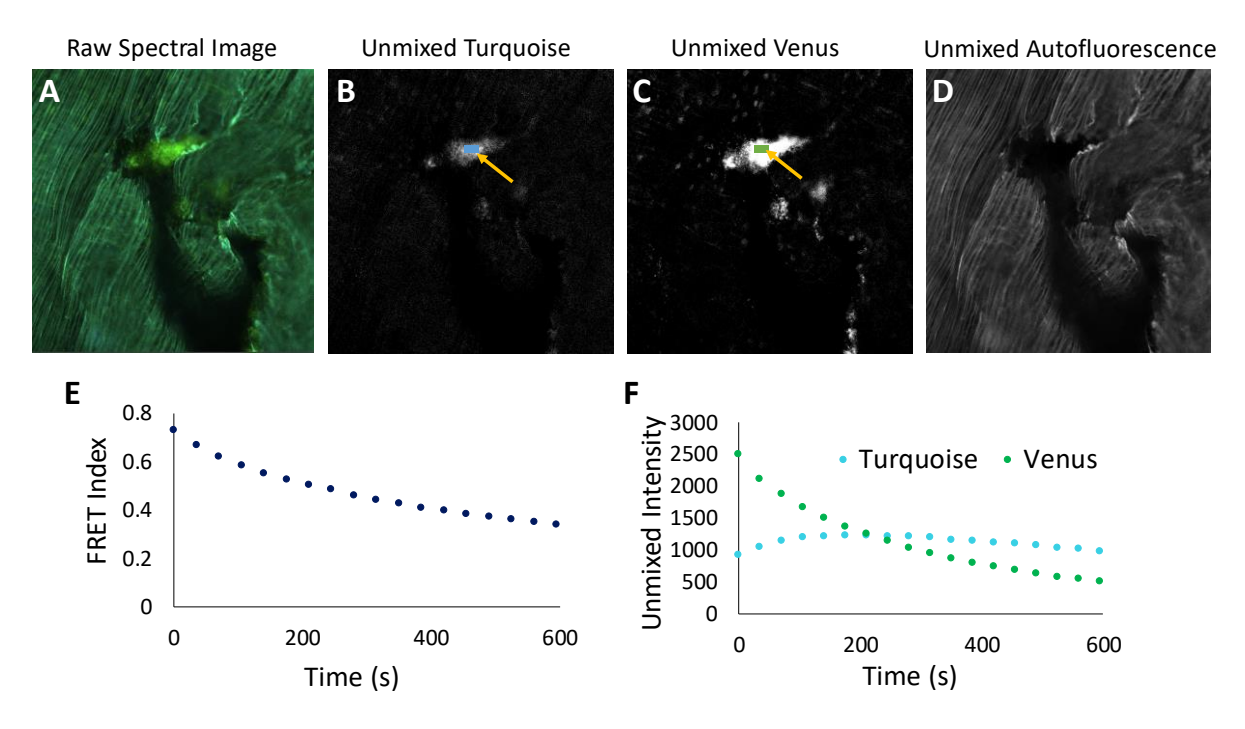


Figure 4: Spectral image data of a resected inferior vena cava (IVC) preparation from the H187 cAMP FRET reporter rat. Raw, false-colored spectral image data from wildtype (A) was unmixed using a spectral library that was customized to the specific tissue type, in this case IVC. Unmixed images of the donor (turquoise, B) and acceptor (venus, C) revealed localized areas, or patches, of FRET-expressing endothelial cells. Unmixed autofluorescence (D) was primarily associated with the basal lamina. Treatment with 50 μ M forsklin and 10 μ M rolipram resulted in decreased FRET index (E), which was further confirmed by visualizing an increase in turquoise and decrease in venus intensity (F).

4. FUTURE WORK

Future work will focus on refinement of tissue preparation and imaging techniques, as well as microscopy settings, to fully optimize the sensitivity for detecting the cAMP FRET reporter in the midst of strong tissue autofluorescence. In addition, work is ongoing in developing alternative spectral imaging microscope platforms that may also provide enhanced sensitivity for detecting the FRET reporter.

5. ACKNOWLEDGEMENTS

This work was supported in part by funding through NIH grant numbers UL1 TR001417, P01 HL066299, NSF grant number 1725937, the Abraham Mitchell Cancer Research Fund, the University of Alabama at Birmingham Center for Clinical and Translational Science (CCTS), and the Economic Development Partnership of Alabama. Drs. Leavesley and

Rich disclose financial interest in a start-up company, SpectraCyte LLC, founded to commercialize spectral imaging technologies.

REFERENCES

- [1] Agarwal, S.R., Miyashiro, K., Latt, H., Ostrom, R.S., and Harvey, R.D., "Compartmentalized cAMP responses to prostaglandin EP2 receptor activation in human airway smooth muscle cells," British Journal of Pharmacology 174(16), 2784–2796 (2017).
- [2] Blackman, B.E., Horner, K., Heidmann, J., Wang, D., Richter, W., Rich, T.C., and Conti, M., "PDE4D and PDE4B function in distinct subcellular compartments in mouse embryonic fibroblasts," Journal of Biological Chemistry 286(14), 12590–12601 (2011).
- [3] Horvat, S.J., Deshpande, D.A., Yan, H., Panettieri, R.A., Codina, J., DuBose, T.D., Xin, W., Rich, T.C., and Penn, R.B., "A-kinase anchoring proteins regulate compartmentalized cAMP signaling in airway smooth muscle," The FASEB Journal 26(9), 3670–3679 (2012).
- [4] Feinstein, W.P., Zhu, B., Leavesley, S.J., Sayner, S.L., and Rich, T.C., "Assessment of cellular mechanisms contributing to cAMP compartmentalization in pulmonary microvascular endothelial cells," American Journal of Physiology-Cell Physiology 302(6), C839–C852 (2012).
- [5] Klarenbeek, J., Goedhart, J., van Batenburg, A., Groenewald, D., and Jalink, K., "Fourth-Generation Epac-Based FRET Sensors for cAMP Feature Exceptional Brightness, Photostability and Dynamic Range: Characterization of Dedicated Sensors for FLIM, for Ratiometry and with High Affinity," PloS one 10(4), (2015).
- [6] Annamdevula, N.S., Sweat, R., Griswold, J.R., Trinh, K., Hoffman, C., West, S., Deal, J., Britain, A.L., Jalink, K., et al., "Spectral imaging of FRET-based sensors reveals sustained cAMP gradients in three spatial dimensions," Cytometry Part A 93(10), 1029–1038 (2018).
- [7] Annamdevula, N.S., Sweat, R., Gunn, H., Griswold, J.R., Britain, A.L., Rich, T.C., and Leavesley, S.J., "Measurement of 3-Dimensional cAMP Distributions in Living Cells using 4-Dimensional (x, y, z, and λ) Hyperspectral FRET Imaging and Analysis.," Journal of Visualized Experiments: Jove(164), (2020).
- [8] Leavesley, S.J., and Rich, T.C., "FRET: Signals hidden within the noise," Cytometry Part A (2014).
- [9] Leavesley, S.J., and Rich, T.C., "Overcoming limitations of FRET measurements.," Cytometry Part A 89(4), 325–327 (2016).
- [10] Leavesley, S.J., Annamdevula, N., Boni, J., Stocker, S., Grant, K., Troyanovsky, B., Rich, T.C., and Alvarez, D.F., "Hyperspectral imaging microscopy for identification and quantitative analysis of fluorescently-labeled cells in highly autofluorescent tissue," Journal of Biophotonics 5(1), 67–84 (2012).
- [11] Levy, S., Wilms, C.D., Brumer, E., Kahn, J., Pnueli, L., Arava, Y., Eilers, J., and Gitler, D., "SpRET: Highly sensitive and reliable spectral measurement of absolute FRET efficiency," Microscopy and Microanalysis 17(02), 176–190 (2011).
- [12] Leavesley, S.J., Britain, A., Cichon, L.K., Nikolaev, V.O., and Rich, T.C., "Assessing FRET using spectral techniques," Cytometry Part A 83(10), 898–912 (2013).
- [13] Garini, Y., Young, I., and McNamara, G., "Spectral imaging: principles and applications," Cytometry Part A 69(8), 735–747 (2006).
- [14] Li, Q., He, X., Wang, Y., Liu, H., Xu, D., and Guo, F., "Review of spectral imaging technology in biomedical engineering: achievements and challenges," Journal of biomedical optics 18(10), 100901–100901 (2013).